11th World Congress on Computational Mechanics (WCCM XI)
5th European Conference on Computational Mechanics (ECCM V)
6th European Conference on Computational Fluid Dynamics (ECFD VI)
E. Oñate, J. Oliver and A. Huerta (Eds)

MODELING FAILURE USING THE CONVECTIVE PARTICLE DOMAIN INTERPOLATION METHOD IN A SHOCK PHYSICS HYDROCODE

SHANE C. SCHUMACHER[1] AND KEVIN P. RUGGIRELLO[2]

[1]Sandia National Laboratories*
PO Box 5800 MS-0836
Albuquerque, NM 87185-0836
scschum@sandia.gov

[2] Sandia National Laboratories*
PO Box 5800 MS-0836
Albuquerque, NM 87185-0836
kruggir@sandia.gov

Key words: MPM, Failure, Shock, Hydrodynamics

Summary
The modeling of failure in a finite volume shock physics computational code poses many challenges. We recently improved upon our recently implemented numerical technique the Material Point Method (MPM) by adding the Convective Particle Domain Interpolation (CPDI) to our finite volume shock physics computational code CTH. The CPDI technique improves accuracy and efficiency of the MPM for problems involving large tensile deformations and rotations. CPDI provides a method for the particles to remain in communication with each other by expanding the interpolation domain over that of the generalized MPM method. This will in turn prevent numerical fracture where fracture occurs when particles loose communication with one another while under going large tensile deformation. This work will focus on a comparison of the abilities of CPDI and generalized MPM in predicting the penetration of steel into aluminium. Simulations of the experiments will be performed to quantify the two numerical techniques.

*Sandia National Laboratories is a multi-program laboratory managed and operated by Sandia Corporation, a wholly owned subsidiary of Lockheed Martin Corporation, for the U.S. Department of Energy's National Nuclear Security Administration under contract DE-AC04-94AL85000.

1 INTRODUCTION

Recently marker methods have been added to a computational shock physics hydrocode named CTH. The marker methods include the Material Point Method (MPM)[1] and

Convective Particle Domain Interpolation (CPDI) [2] as methods of modeling fields as Lagrangian in CTH. The integration of the Lagrangian numerical methods expands the capabilities of CTH for solid material modeling, structural applications and fluid-structure interaction to name a few applications. The marker methods have also been integrated into the existing CTH parallel and Adaptive Mesh Refinement (AMR) frameworks allowing for massively parallel computational simulations. With the large capacity for computations, accuracy is also improved where the state of the material or structure is affected by Eulerian remap (advection) processes. Just as AMR increases the accuracy of simulations by providing refinement where needed, the inclusion of the marker methods increases accuracy through Lagrangian numerical methods.

The marker methods are built upon Lagrangian numerical concepts, therefore the marker fields do not use the Eulerian advection processes. Previously, CTH was a pure Eulerian computational shock physics hydrocode. This entails a numerical cycle that includes a Lagrangian step with a remap step (advection) that forms the Eulerian numerical method. When using the marker methods, the remap step for a marker field is not necessary and therefore not performed for the marker field within a CTH computational cycle. Another benefit of the marker method is that it utilizes the existing constitutive models within CTH. The material model physics are the same whether used in CTH or with markers.

Specifically, MPM and CPDI provide mechanisms for modeling fracture mechanics within CTH. Previously the only method of fracturing fields was through void insertion. With the MPM and CPDI methods damage, fracture, etc. are stored on the marker itself. Therefore, quantities of damage or other field state variables may dictate the individual marker failure. Once the marker fails, the marker may be switched to another marker or CTH material that is hydrodynamic or non-shear supporting. This non-shear supporting material may fracture once again using CTH void insertion. This will occur if the failed material experiences a tensile state further in the analysis.

2 METHODOLOGY

The marker methods are in essence a particle method, but defined here as a marker, where a marker “marks” the material or field presence in the computational cell. The marker presence is defined as the state of the marker based on mass, location, velocity, extra (state) variables, etc.. The markers do not communicate between each other and instead use a background grid to track and communicate between each other, whether Eulerian (CTH fields) or other marker fields. The collection of markers moves according to the center of mass of the field. The state of the field is interpolated between the marker field and the background grid for interaction with other fields.

The marker numerics are broken into two processes that are coupled, the hydrodynamic state and the strength state of the field. The fluid behavior entails the field variables, pressure P, temperature T, energy E, specific volume ν and the state or extra hydrodynamic variables denoted as *eos. The hydrodynamic state of the field is computed on the CTH background grid. The strength behavior entails the stress σ or the deviatoric stress state σ' and the state or

extra variables *. The strength of the marker field is computed using the Material Point Method. The marker methods utilize the strength of two numerical techniques, Eulerian for the hydrodynamic behavior and Lagrangian for the strength and failure of the field. An important note is that the hydrodynamic state of the field is updated to the marker field after the Equation of State (EOS) computation at the bottom of each cycle, denoted as n (where n is the current cycle number). This is a complete rewrite or reset of the marker field based on the background EOS grid data. In CTH, the EOS computation is performed at the bottom of the cycle (n) to compute the new pressure for the (n+1) cycle. Fracture in CTH is performed at the bottom of cycle (n) after the EOS update.

The Material Point Method (MPM) is based on Fluid-Implicit-Particle (FLIP) [3] but with the addition of strength mechanics on the markers. The implementation of MPM in CTH is performed by interpolating data between the marker field and the CTH grid. The CTH grid is used to communicate between fields either MPM or CTH. MPM computes accelerations from the marker field and the results are communicated to the grid vertices. The mixing of the field accelerations is performed at the grid vertices, where all materials in the computation are mixed conserving momentum. By definition, CTH uses a single velocity field with non-equilibrium field pressures, temperatures, energies and densities. Therefore, all materials have the same velocity at a vertex and/or cell face. A detailed summary of the marker numerical implementation process in CTH is found under Schumacher et. al. [4].

The original MPM method suffers from cell crossing noise due to the lack of smoothness of the shape functions, and "numerical fracture" when the markers become separated by more than a grid cell. To alleviate the cell crossing noise Bardenhagen etal.[5] introduced the Generalized Interpolation Material Point (GIMP) method, which allows the marker domains to deform aligned with the background grid and constructs smooth shape functions. However the GIMP method does not capture the rotation of the marker domains. The CPDI method allows the marker domains to deform as parallelograms and constructs smooth basis functions on the grid. The CPDI method has been shown to simulate large deformation problems accurately and alleviates the cell crossing noise present in the standard MPM. Since the GIMP and CPDI methods allow the marker domains to stretch across multiple cells, their basis functions can have non-local support during massive deformation problems.

In the CPDI method, a marker is initially defined as a parallelogram, which is deformed during the calculation. The deformation is tracked through the temporal integration of the deformation gradient tensor, which maps the undeformed marker domain to the deformed domain. Figure 1 shows an initial marker domain dimensioned by r_1^0 and r_2^0 and Fig. 2 shows the updated parallelogram marker domain at time step n + 1. The marker domain is determined according to,

$$\vec{r}_1^{n+1} = \bar{F}_p^{n+1}\vec{r}_1^0 \qquad (1)$$
$$\vec{r}_2^{n+1} = \bar{F}_p^{n+1}\vec{r}_2^0.$$

The basis functions are evaluated at the marker domain corners, allowing the marker to stay

connected to its neighbors even during large strains where it can potentially span multiple cells.

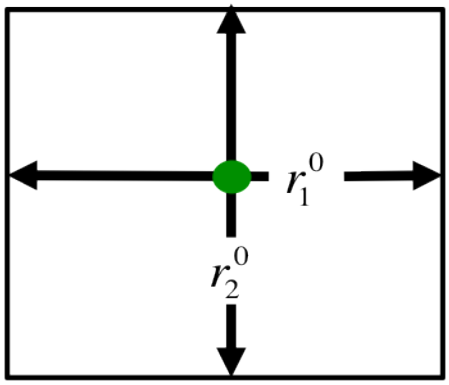

Figure 1. Initial marker domain

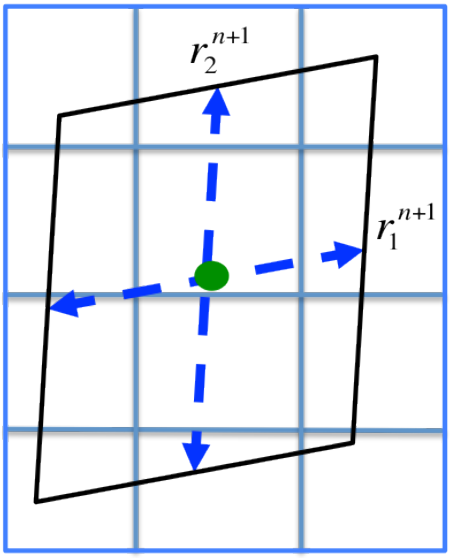

Figure 2. Update marker domain at cycle n+1

3 EXAMPLE

An example demonstrating the failure methodology is the penetration of a 6061-T6511 aluminum block by a 4340 sound nose steel penetrator [6]. The aluminum target is a cylinder, 25 cm diameter x 30 cm length. The penetrator is 4340 vacuum-arc remelted (VAR) spherical nose cylindrical penetrator, body of 7.11 mm diameter x 71.1 mm length. The spherical nose is 7.11 diameter making the total penetrator length of 74.655 mm length from tip to tail. Tests were performed at several velocities with depth of penetration, pitch and yaw all recorded for each experiment. The experiment chosen below is at 841 m/s with 0 pitch and 0 yaw. The depth of penetration from the experiment was measured at 91 mm into the

target. The simulation was setup axis symmetric where the pitch and yaw are 0 respectively. The simulation mesh size is 1 mm x 1 mm, with 16 markers per cell, giving 4,592 markers in the penetrator and 600,000 markers in the target. Typical runtime for the solution is approximately 30 minutes in serial. Convergence of the solution was determined by altering the grid size and marker counts per cell where the solution presented below is adequately converged.

The results are shown below, in Figure 3 the initial example problem setup is shown. Figure 4 shows the final penetration depth of the penetrator into the target. The unfailed materials are blue for the steel and gray for the aluminum target. The failed material is red for the steel and brown for the aluminum. From the simulation, ejecta are seen leaving the target, primarily aluminum material. The current penetrator to target interaction is fully coupled or "welded" based on the single velocity field within CTH. Therefore, premature failure/oblation of the penetrator is seen at the interface. This is evident from degradation of the aluminum target. The depth of penetration from the experiment was measure at 91 mm. The simulation results agree well with the experimental results at ~98 mm.

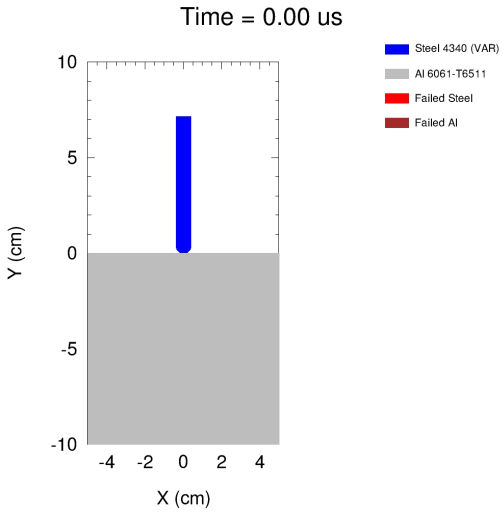

Figure 3. Example Problem Setup, 6061-T6511 Target and 4340 VAC penetrator.

The next result shown below, in Figure 5 is using CPDI for the penetrator and target. The depth of penetration for the CPDI case is ~91 mm coming the closest to the experimental results. The unfailed materials are blue for the steel and gray for the aluminum target. The failed material is red for the steel and brown for the aluminum. From the simulation, ejecta are seen once again leaving the target, primarily aluminum material. The current penetrator to target interaction is fully coupled or "welded" based on the single velocity field within CTH. Once again, premature failure/oblation of the penetrator is seen at the interface. This is evident from degradation of the aluminum target. The marker and cell counts remained the same where convergence was found at similar values as the MPM simulation above. The CPDI computation took approximately 50 minutes to complete. The numerical computations

are more with CPDI when interpolating or computing field derivatives therefore obtaining longer runtimes is expected.

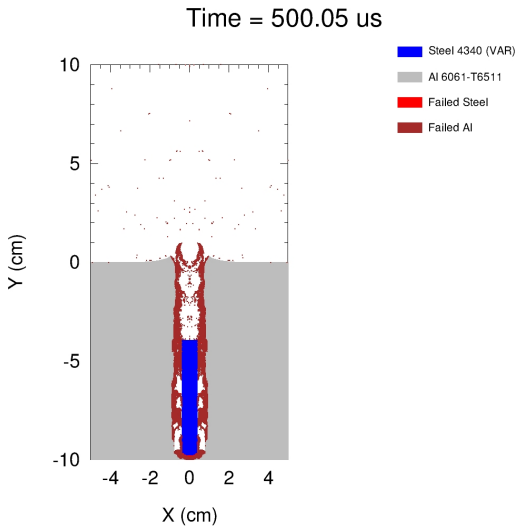

Figure 4. Penetration of 6061-T6511 Target by a 4340 VAC penetrator @ 500 μs using MPM.

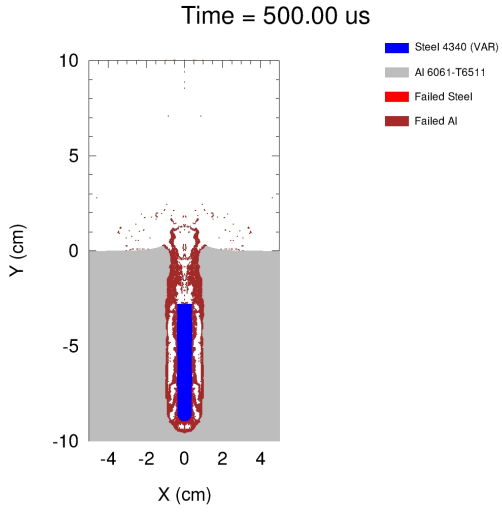

Figure 5. Penetration of 6061-T6511 Target by a 4340 VAC penetrator @ 500 μs using CPDI.

4 CONCLUSION

Two methods of the Material Point Method (MPM) are described above, the original MPM and the Convective Particle Domain Interpolation (CPDI) method. Both methods, called marker methods, reside in a computation shock physics tool named CTH. A brief overview of the marker methods in CTH is provided above with the appropriate references for further reading. A simple penetration example of steel and aluminum is chosen where both methods

are used to simulate the event. Both methods provide good results as compared to experimental data, where the MPM resulted in ~98 mm penetration depth and CPDI resulted in ~91 mm penetration depth. The experiments showed a depth of penetration to be at 91 mm. The MPM solution was complete in 30 minutes as compared to the CPDI solution at 50 minutes. The results also show the oblation of the target and penetrator that was not seen in the experiments. This is attributed to the "welded" interface and soft aluminum material properties, where a common velocity is determined in the mixed cell. Numerical techniques exist in CTH to simulate slip or friction boundary conditions, but these numerical techniques are not compatible with the marker methods. Therefore soft aluminum material properties were used for a lesser strength aluminum to approximate the depth of penetration.

REFERENCES

[1] Sulsky, Deborah, Chen Z. and Schreyer, Howard L., A Particle Method for History-Dependent Materials, Computational Methods Applied Mechanical Engineering, 118, 179-196, (1994)

[2] A. Sadeghirad, R.M. Brannon and J.Burghardt, A convective particle domain interpolation technique to extend the applicability of the material point method for problems involving large deformations.

[3] Brackbill, J.U. and Ruppel, H.M., FLIP: A Method for Adaptively Zoned, Particle-In-Cell Calculations of Fluids in Two Dimensions, Journal of Computational Physics, 65, 314-343 (1986)

[4] Schumacher, S.C., Ruggirello, K.P. and Kashiwa, B., CTH Marker Lagrangian Capabilities, 83rd Shock and Vibration Exchange, New Orleans, LA, November 4-8, 2012

[5] S. Bardenhagen and E. Kober, The generalized interpolation material point method, CMES, Comput. Model. Engrg. Sci. vol. 5, pp. 477-495, 2004

[6] Forrestall, M. J. and Piekutowski, A. J., Penetration Experiments with 6061-T6511 Aluminum Targets and Spherical-Nose Steel Projectiles at Striking Velocities Between 0.5 and 3.0 km/s, International Journal of Impact Engineering, 2000, 24, 57-67